# Field confinement and quality factor of the multilayer cavity resonators

N. Yogesh and V. Subramanian[a)]
*Microwave Laboratory, Department of Physics, Indian Institute of Technology Madras, Chennai-600 036, India*

(Received 3 September 2011; accepted 31 October 2011; published online 12 December 2011)

The field confinement aspect of a multilayer cavity resonator formed by a one-dimensional photonic crystal with prism wedge configuration is described in this paper. The prism wedge consists of alternating dielectric layers and is used for the construction of polygon multilayered structures with different symmetries like $C_{4v}$-square and $C_{6v}$-hexagon. Field confinement is studied by finding the resonant modes and quality factors ($Q$) of the proposed geometries. The computed $Q$ factors for the two-dimensional geometries (the third dimension is taken to be infinity) are of the order of $10^3$–$10^7$. On the other hand, for the finite height of the cavity, the estimated $Q$ factor is found to be of the order of $10^4$. An attempt has been taken to achieve the vertical confinement of light for a few of the resonant modes so that the proposed cavities may be implemented for microwave applications, especially in spectroscopic techniques. © *2011 American Institute of Physics*. [doi:10.1063/1.3667292]

## I. INTRODUCTION

Photonic crystals (PC) are useful for the storage of electromagnetic (e-m) radiation in the form of cavity resonating structures.[1] The cavities made of PC can be based on either the bandgap effect[2] or the anomalous dispersion.[3,4] The simplest form is to create the defect sites in regular periodic patterns, which uniquely support the specific e-m modes at the bandgap frequencies.[5–8] The recent efforts in the realization of cavities report ultrahigh quality factor along with small mode volumes[9–14] and explore the possible applications ranging from field confinement to laser cooling.[15,16]

In this paper, two structures based on the square and hexagon multilayer configuration (Fig. 1) are presented to understand the field confinement effect. It may be noted from Fig. 1 that the basic element of the proposed geometries is the prism wedge, whose constituents are periodic in one dimension (1D). It is well known that the 1D layer will act as a perfect mirror at the bandgap frequencies.[17] One can use this concept to construct the polygon structure with different structural symmetries like $C_{4v}$-square, and $C_{6v}$-hexagon for the confinement of e-m waves. For example, the $C_{4v}$ symmetry cavity is constructed by four 45° prism wedges and each prism consists of periodic alternating dielectric layers of alumina slab (relative dielectric permittivity is 9.0) of width 0.3 a and air spacing of 0.7 a (where a is the lattice constant).

## II. *Q* FOR AN INFINITE HEIGHT CAVITY—TWO-DIMENSIONAL CALCULATIONS

Initially, attention has been paid to the field confinement effect for the modes that are not allowed by the multilayer. Figure 2 shows the in-plane band structure of the 1D multilayer (obtained through plane wave method based free e-m solver MPB),[18] where the first bandgap spans from 0.209 to $0.403(2\pi c/a)$. Because the presented cavity's center space (−0.7a to 0.7a) is surrounded by the multilayer, the in-plane propagation is effectively forbidden at the bandgap frequencies for an e-m source excited at the center of the cavity. However, it is necessary to mention that the cavity geometry also has sharp corners and because of this, off-axis propagation may exist via the corner of the cavity. For example, the off-axis band structure (transverse magnetic (TM) polarization) of the 1D multilayer given in Fig. 2(b) does not show the complete bandgap and, hence, fields can even be allowed for certain $k_x$ and $k_y$ values. Therefore, it is possible to expect that the in-plane field confinement offered by the number of multilayered sides may be limited by the off-axis propagation (leakage) due to the number of vertices.

To show this, the resonant modes, their decay nature, and quality factors are found through 2D calculations (where the height of the cavity is taken to be infinity) using the finite-difference time-domain (FDTD) method based free e-m solver MEEP.[19] The basic idea is to pump energy into the cavity and observe the decay process. In order to do so, the Gaussian pulse centered on the $0.311(2\pi c/a)$ with the pulse

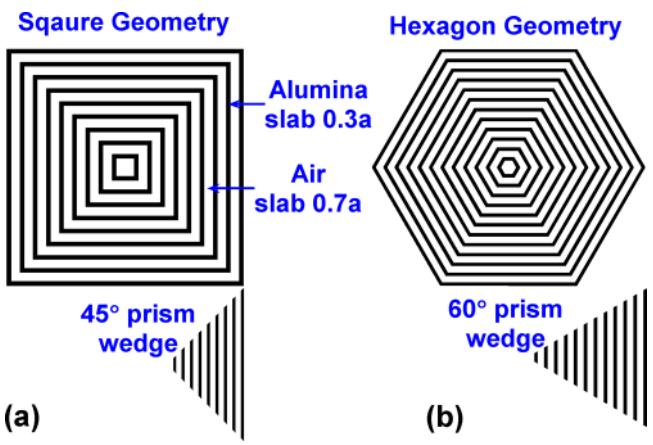


FIG. 1. (Color online) Proposed multilayered cavity geometries. (a) Square-$C_{4v}$ symmetry; (b) hexagon-$C_{6v}$ symmetry.

[a)]Author to whom correspondence should be addressed. Electronic mail: manianvs@iitm.ac.in.

 

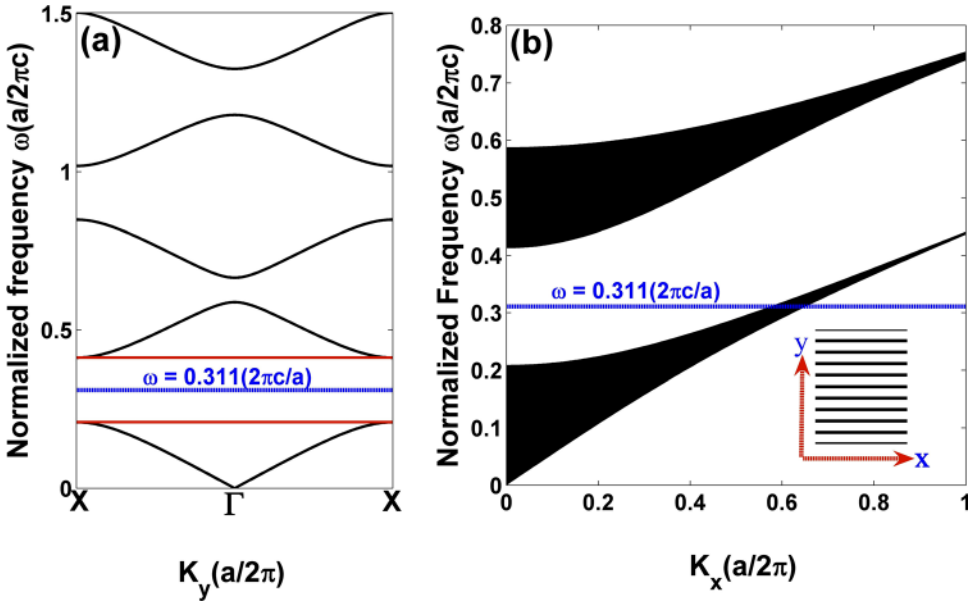


FIG. 2. (Color online) (a) In-plane band structure of the 1D PC consists of alternative layers of alumina slab (0.3a) and air medium (0.7a). The first bandgap is shown with solid horizontal lines. (b) Projected band structure corresponding to the TM polarization for the first two bands. The midgap frequency $0.311(2\pi c/a)$, given with the dotted line, is allowed in certain $k_x$ and $k_y$ values.

width of $0.2(2\pi c/a)$ is excited at the center of the cavity. The choice of this frequency excitation is based on the in-plane bandgap information of the 1D multilayer given in Fig. 2(a). (Hence, the calculation is restricted only to the resonant modes within the forbidden regime of the 1D multilayer and the other modes of the cavity are not considered. If one wants to solve the complete band structure information, one may consider the super-cell treatment for the cavity. For example, in fiber optics, the band spectrum of the cylindrical multilayer is well known.)[20]

To solve for the resonant modes, the computational domain is surrounded by the perfectly matched boundary layers (absorbing layers)[21] and transverse magnetic polarization ($E_z$ component) is assigned to the excitation source. After the excitation and complete decay of the pulse, the field values present at the center of the resonator are taken for the extraction of the resonant modes. For this purpose, a filter diagonalization method[22] is employed through HARMINV.[22,23]

Harminv analyzes the field $f(t)$ at a given point and expresses it as a sum of the modes as $f(t) = \sum a_n exp(-i\omega_n t)$ for the specified frequency bandwidth. Here $a_n$ is the complex amplitudes and $\omega_n$ is the complex frequencies. The $Q$ factor is calculated through the expression as,

$$Q = \frac{Re(\omega)}{-2\,Im(\omega)}. \tag{1}$$

Here $Q$ is the computed quality factor, $Re(\omega)$ is the real part of the complex frequencies, and $Im(\omega)$ is the imaginary part of the complex frequencies (corresponds to the decay rates of the resonant modes). For the accurate calculation of the $Q$ factor, one need apply the HARMINV only after the complete decay of the Gaussian pulse. For example, the $Q$ factors of the square and hexagonal configurations given in Table I are calculated after 50 000 time units of the complete decay of the pulse. For the fixed number of photonic layers (9 layers for square and 12 layers for hexagon), the $Q$ factors are obtained in the range of $10^3$–$10^7$ for the proposed geometries and their respective mode patterns are given in Fig. 3. It is evident from Fig. 3 that the center cavity space specifically supports the resonant modes and some of them are even confined in the dielectric layer. For example, the mode at $0.36662(2\pi c/a)$ for a square cavity is confined around the dielectric so that it has a very low decay rate and has a high $Q$ factor of the order of $10^7$.

However, it may be noted that these calculations are only for two dimensions, where the height of the cavity is taken to be infinity. As long as the height is being ignored, the reported $Q$ values will only indicate the in-plane field confinement. In reality, any photonic cavity has at least two energy decay channels; the one being considered as the in-plane losses ($Q_{in\text{-}plane}$) and the other one being the out-of-plane losses ($Q_{out\text{-}of\text{-}plane}$) and the total $Q$ factor ($Q_{total}$) comprises both the losses, as per Eq. (2),

$$\frac{1}{Q_{total}} = \frac{1}{Q_{in\text{-}plane}} + \frac{1}{Q_{out\text{-}of\text{-}plane}}. \tag{2}$$

By examining Eq. (2), it can be justified that the $Q_{total}$ approaches $Q_{out\text{-}of\text{-}plane}$ when $Q_{in\text{-}plane}$ is arbitrarily very large. Because 2D calculations for an infinite height cavity only indicate the $Q_{in\text{-}plane}$, practical applications of these geometries require the estimation of $Q$ for the finite dimensional structures.

TABLE I. List of computed $Q$ factors.

| Square Configuration | | Hexagonal Configuration | |
|---|---|---|---|
| Resonant frequencies $\omega$ in $(2\pi c/a)$ | Quality factor $Q$ | Resonant frequencies $\omega$ in $(2\pi c/a)$ | Quality factor $Q$ |
| 0.29159 | $3.52 \times 10^4$ | 0.26004 | $1.09 \times 10^7$ |
| 0.29748 | $1.07 \times 10^6$ | 0.38221 | $5.36 \times 10^7$ |
| 0.36662 | $3.13 \times 10^7$ | 0.40291 | $3.74 \times 10^5$ |
| 0.40032 | $8.22 \times 10^4$ | 0.40577 | $4.71 \times 10^6$ |

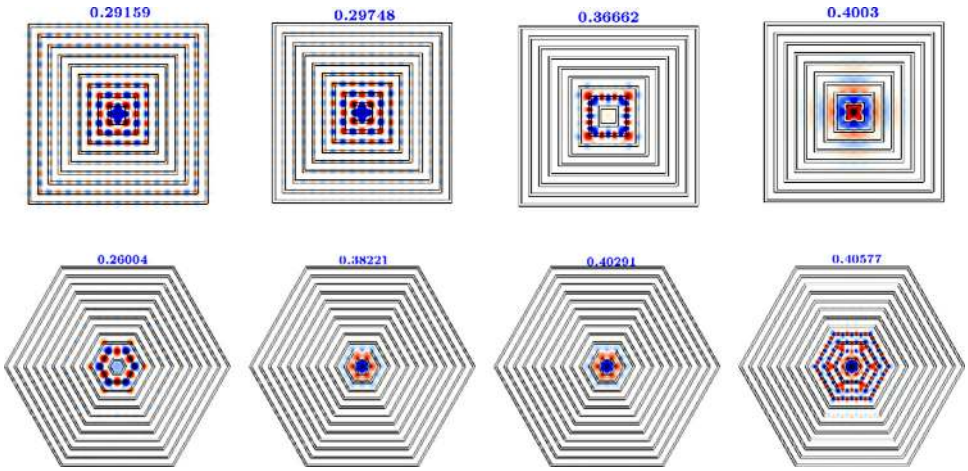


FIG. 3. (Color online) $E_z$ field patterns of the resonant modes of the square and hexagon cavities. In all cases, the field pattern is simulated with short Gaussian pulse with frequency width of 0.05 ($2\pi c/a$). The center frequencies are specified at the top of the geometries. For the square case, the field pattern is captured at 500 time units and for the hexagon, the field pattern is captured at 1500 time units.

## III. ESTIMATION OF *Q* FOR A THREE-DIMENSIONAL CAVITY

$Q$ factor for a finite height (3D) square cavity is estimated using the transient analysis based FDTD e-m solver CST MICROWAVE STUDIO.[24] With respect to the 2D calculations, two important changes are considered. The calculations are performed with specific microwave length-scales (cm) rather than the normalized units. The theoretical point source used in 2D computation is replaced with the monopole source in the microwave regime. The cavity given in Fig. 4 has 9 layers with the finite height of 10 cm. The computational domain is surrounded with open boundaries except at the bottom of the cavity. The bottom is the ground plane so that the monopole of length $\lambda/4$ can be fed by the discrete current source, as shown in Fig. 4. To verify the 2D calculations, the mode at $0.36662(2\pi c/a)$ is taken owing to their high $Q$ value. For the microwave-length scale of $a = 1$cm, this normalized angular frequency $\omega = 0.36662\left(\frac{2\pi c}{a}\right)$ corresponds to the linear frequency of 10.999 GHz and, hence, the short Gaussian pulse with range of 10.96 GHz to 11.06 GHz is considered for the excitation.

To find out the resonant frequency, electric field inside the cavity is monitored using the point probe. The intrinsic $Q$ factor of the cavity can be found through watching the energy

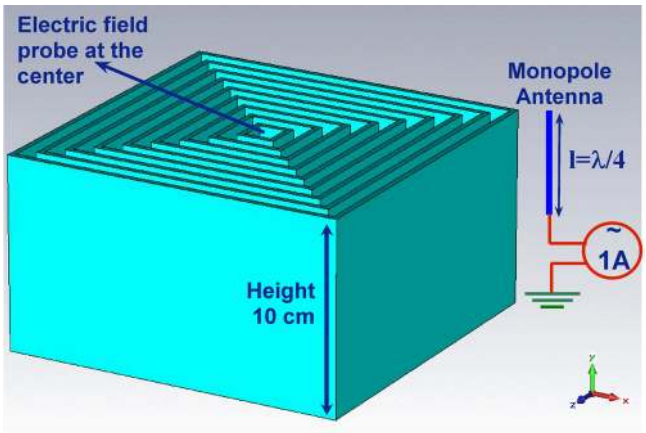


FIG. 4. (Color online) Finite height of the cavity. A monopole source is used for the TM polarization excitation. Point probe is placed at the center of the cavity for detecting the resonant frequency.

decay of the pulse and it is given in Fig. 5(a). It is clear that after the excitation of the short pulse, the energy decays very slowly. The complete decay will take exceptional computational time and memory and because of this, the calculation is aborted after solving a few pulse widths. The recorded power spectrum (Fourier transformation of time-domain signals) is given in Fig. 5(b). Similar to the 2D calculations, a higher order filter is applied to extract the resonant mode and it is shown with red solid circles in Fig. 5(b). The resonant mode frequency found from the probe spectrum is 11.02624 GHz. The corresponding decay rate $\left(\frac{dE}{dt} = 0.00919\left(\frac{dB}{ns}\right)\right)$ can be calculated from the slope of the energy curve, which is given in the inset of Fig. 5(a). The expression for $Q$ factor in terms of energy decay rate is given as,

$$Q_{intrinsic} = \frac{\omega_0.10}{\ln(10).\frac{dE}{dt}\left[\frac{dB}{ns}\right]}, \tag{3}$$

where $Q_{intrinsic}$ (Ref. 25) is the intrinsic quality factor of the cavity, $\omega_0$ is the angular resonance frequency, and $\frac{dE}{dt}$ is the energy decay rate expressed in dB per nano-second. Substituting their respective values in Eq. (3), one can find the value of $Q_{intrinsic}$ to be $3.274 \times 10^4$. The corresponding electric field ($E_y$ component—here y is the axial direction, rather than z in 2D calculations) pattern at $f_o = 11.02624$ GHz given in Fig. 5(c) matches with the mode profile obtained through the 2D calculations. This estimated $Q$ value for a 3D cavity reveals the role of finiteness of the system along the third dimension and shows the importance of the out-of-plane radiation losses with respect to the 2D calculations.

## IV. VERTICAL CONFINEMENT

This section reveals the task of confining the light along the third dimension so that one can improve the $Q$ factor further. To demonstrate the vertical confinement of light, the resonant mode of the square cavity at $\omega = 0.4003\left(\frac{2\pi c}{a}\right)$ is taken (one can refer to Fig. 3). The reason for this choice is that it has a single mode behavior and fields are concentrated at the center. Hence, discussing the confinement mechanism of this mode will be useful for practical applications.

Figure 6 shows the results of vertical confinement of light. First it is observed from 2D calculation that the mode

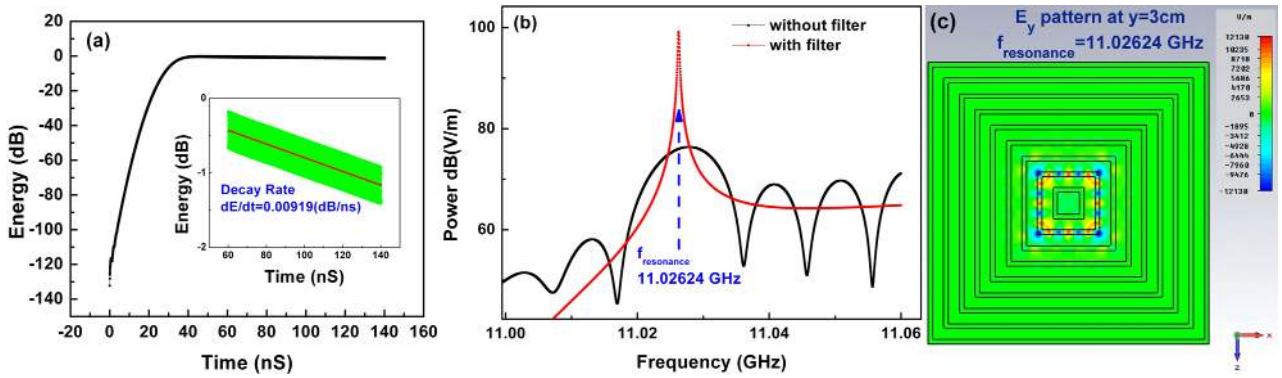


FIG. 5. (Color online) (a) Energy decay scheme. Inset shows the tail of the energy decay. (b) Power spectrum (Fourier transformation of the time-domain signals) recorded by the point probe. Power spectrum without filtering is given by black solid squares and the filtered spectrum is given by red solid circles. (c) $E_y$ component captured at 3 cm for the resonant frequency of 11.02624 GHz.

at $0.4003(2\pi c/a)$ has a $Q$ factor value of the order of $10^4$. However, for a finite height of the cavity (where all boundaries are opened), the energy decay scheme given with red solid circles in Fig. 6(a) implies a $Q$ factor value of only approximately 1000. This can also be corroborated from the probe signal spectrum given in the inset of Fig. 6(a), where the signal (red solid circles) falls off rapidly as the light simply escapes out of the cavity through top and bottom channels, regardless of the in-plane confinement offered by the surrounding multilayer.

On the other hand, if the top and bottom of the geometry are terminated by a metal layer (a simple way to confine light along three dimensions at microwave length scales; in optics, SOI (silicon on insulator) substrate is usually employed),[26] the out-of-plane radiation loss is reduced drastically and the mode is confined within the center cavity space. This can be verified from the amplitude signals given in the inset of Fig. 6(a), where one can see the number of oscillations (black solid squares), as the amplitude does not decay significantly over a longer time. The intrinsic $Q$ factor calculated from the corresponding energy decay given in Fig. 6(a) is of the order of $10^4$.

Figures 6(b) and 6(c) show the resonant spectra for the open boundaries and metal layers, respectively. By comparing both of them, one can realize the importance of vertical confinement, as the $Q$ factor for the metal layer case is increased by a factor of 10 with respect to the open boundary case. The corresponding $E_y$ field pattern given at 12.1636

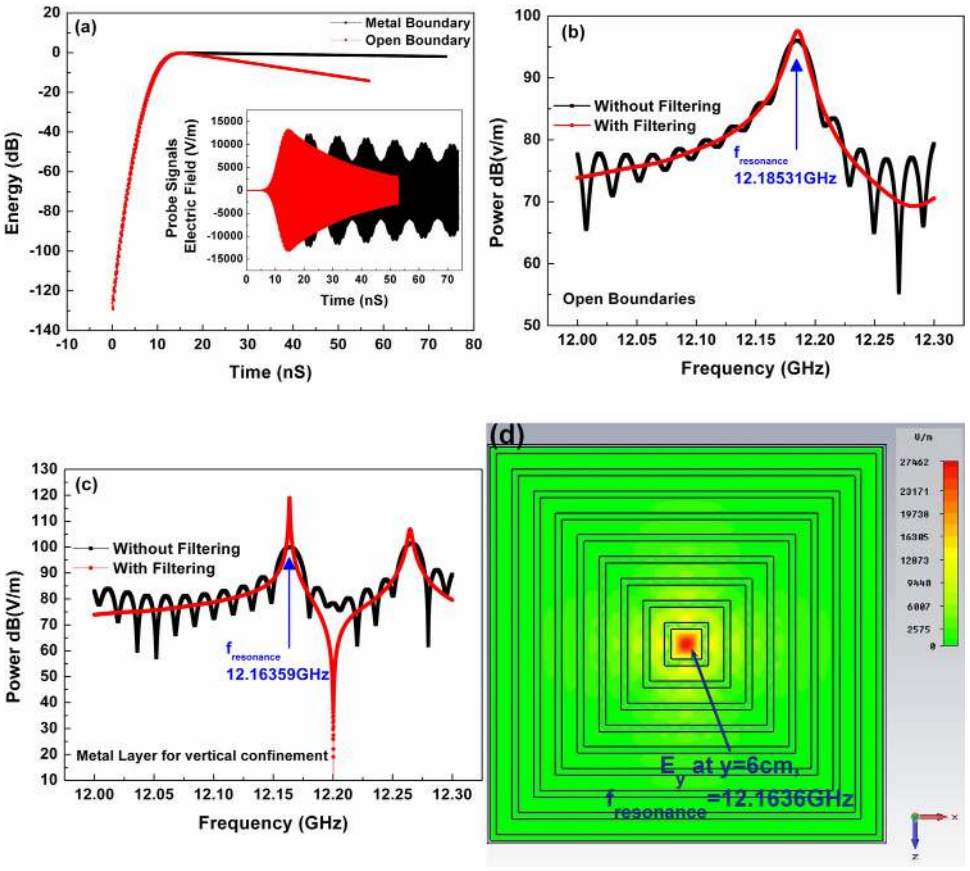


FIG. 6. (Color online) Vertical confinement of light. (a) Energy decay for the open boundaries and metal layers. Inset shows the corresponding time-domain amplitude signals. (b) and (c) show the resonant spectra for the open boundaries and metal layers, respectively. (d). Absolute value of $E_y$ component captured at $y = 6$ cm for the resonant frequency of 12.1636 GHz.

GHz in Fig. 6(d) shows the single mode behavior of the cavity. This task of confining the light at center cavity space has an impact in microwave spectroscopy, as the concentrated field may be used for dielectric/magnetic materials characterization using cavity perturbation techniques, microwave heat treatment of materials, non-destructive evaluation, and so on.

## V. CONCLUSIONS

In summary, the polygon multilayered cavities with different symmetries are proposed in this work and the field confinement aspect is studied numerically. It is verified that the in-plane field confinement has a $Q$ factor of the order of $10^3$–$10^7$. However, for a finite height of the cavity, the $Q$ factor is reduced due to the out-of-plane radiation losses and the estimated value for the multi mode behavior is of the order of $10^4$. The mechanism of vertical confinement is studied for the single-mode behavior of the square cavity. It is demonstrated that by adding up the metal layers along the third dimension, $Q$ factor is improved by a factor of 10 and the fields are concentrated at the center. Owing to the high $Q$ value, the proposed geometry may be employed for microwave sintering (material heating) applications, spectroscopy techniques, and so on.

[1]C. M. Soukoulis, *Photonic Band Gap Materials* (Kluwer, Dordrecht, The Netherlands, 1996), pp. 391–426.
[2]O. Painter, J. Vučković, and A. Scherer, J. Opt. Soc. Am. B. **16**, 275 (1999).
[3]Z. Ruan, and S. He, Opt. Lett. **30**, 2308 (2005).
[4]N. Yogesh and V. Subramanian, Prog. Electromagn. Res. M **12**, 115 (2010).
[5]I. Khromova, R. Gonzalo, I. Ederra, and P. D. Maagt, J. Appl. Phys. **106**, 014901 (2009).
[6]D. Stieler, A. Barsic, G. Tuttle, M. Li, and K.-M. Ho, J. Appl. Phys. **105**, 103109 (2009).
[7]C.-J. Wu, and Z.-H. Wang, Prog. Electromagn. Res. **103**, 169 (2010).
[8]F. Li, J. Liu, and Y. Wu, J. Appl. Phys. **109**, 124907 (2011).
[9]A. R. Md Zain, N. P. Johnson, M. Sorel, and R. M. De La Rue, IEEE Photon. Technol. Lett. **21**, 1789 (2009).
[10]Y. Tanaka, T. Asano, and S. Noda, J. Lightwave Technol. **26**, 1532 (2008).
[11]L. Luo, and C. Jiang, IEEE Symposium on Photonics and Optoelectronics 2010 (Chengdu, China, June 19-21, 2010), pp. 1–3.
[12]Y. Song, M. Liu, Y. Zhang, X. Whang, and C. Jin, J. Opt. Soc. Am. B. **28**, 265 (2011).
[13]T.-W. Lu, L.-H. Chiu, P.-T. Lin, and P.-T. Lee, Appl. Phys. Lett. **99**, 071101 (2011).
[14]M. Davanco, M. T. Rakher, D. Schuh, A. Badolato, and K. Srinivasan, Appl. Phys. Lett. **99**, 041102 (2011).
[15]O. Toader, S. John, and K. Busch, Opt. Express **8**, 217 (2001).
[16]A. Rahmani, and P. C. Chaumet, Opt. Express **14**, 6353 (2006).
[17]K. Sakoda, *Optical Properties of Photonic Crystals*, 2nd ed. (Springer, Berlin, 2005) pp. 1–12 .
[18]S. G. Johnson and J. D. Joannopoulos, Opt. Express **8**, 173 (2001).
[19]A. F. Oskooi, D. Roundy, M. Ibanescu, P. Bermel, J. D. Joannopoulos, and S. G. Johnson Comput. Phys. Commun., **181**, 687 (2010).
[20]J. D. Joannopoulos, S. G. Johnson, J. N. Winn, and R. D. Meade, *Photonic Crystals: Molding the Flow of Light*, 2nd ed. (Princeton University Press, Princeton, NJ, 2008) Chap. IX, 156–189.
[21]A. Taflove and S. C. Hagness, *Computational Electrodynamics: The Finite Difference Time-Domain Method*, 3rd ed. (Artech House, Norwood, MA, 2005) 273–290.
[22]V. A. Mandelshtam and H. S. Taylor, J. Chem. Phys. **107**, 6756 (1997); **109**, 4128 (1998).
[23]For more information about HARMINV, see http://ab-initio.mit.edu/wiki/index.php/Harmiv.
[24]For more information about CST MICROWAVE STUDIO 2010, see http://www.cst.com.
[25]S. Kurennoy, D. Schrage, R. Wood, T. Schultheiss, J. Rathke, and L. Young, Paper presented at the American Physical Society April Meeting, Denver, CO, May 1–4, 2004.
[26]S. Noda and T. Baba, *Roadmap on Photonic Crystals* (Kluwer, Dordrecht, The Netherlands, 2003) Chap. III, pp. 65–74.